BRL

MEMORANDUM REPORT NO. 1709

BASE PRESSURE MEASUREMENTS ON SHARP AND BLUNT 9° CONES AT MACH NUMBERS FROM 3.50 TO 9.20

by

Neil A. Zarin

November 1965

U. S. ARMY MATERIEL COMMAND
BALLISTIC RESEARCH LABORATORIES
ABERDEEN PROVING GROUND, MARYLAND

Destroy this report when it is no longer needed.
Do not return it to the originator.

The findings in this report are not to be construed as an official Department of the Army position, unless so designated by other authorized documents.

The use of trade names or manufacturers' names in this report does not constitute indorsement of any commercial product.

B A L L I S T I C R E S E A R C H L A B O R A T O R I E S

MEMORANDUM REPORT NO. 1709

NOVEMBER 1965

1. Cones -- Base pressure
2. Base pressures -- measurement
1 - V

BASE PRESSURE MEASUREMENTS ON SHARP AND BLUNT 9° CONES AT MACH NUMBERS FROM 3.50 TO 9.20

Neil A. Zarin

Exterior Ballistics Laboratory

RDT&E Project No. 1A222901A201

A B E R D E E N P R O V I N G G R O U N D, M A R Y L A N D

B A L L I S T I C R E S E A R C H L A B O R A T O R I E S

MEMORANDUM REPORT NO. 1709

NAZarin/gk
Aberdeen Proving Ground, Md.
November 1965

BASE PRESSURE MEASUREMENTS ON SHARP AND BLUNT 9° CONES AT MACH NUMBERS FROM 3.50 TO 9.20

ABSTRACT

Base pressure measurements were made on sharp and hemispherically blunted 9° cones at Mach numbers from 3.50 to 9.20. The tests were carried out in the Ballistic Research Laboratories' Supersonic and Hypersonic Wind Tunnels at Aberdeen Proving Ground, Maryland. The data obtained are compared to experimental data and to data from semiempirical analyses from other sources. An empirical correlation for the base pressure data is presented. The relative contributions of base and form drag to total drag are compared.

TABLE OF CONTENTS

INDEX TO ILLUSTRATIONS

DEFINITION OF SYMBOLS

C_D	Drag coefficient = $\frac{D}{q\,S}$
D	Drag force
k	Constant used in base pressure coefficient correlation equation
ℓ	Model wetted length
M_∞	Free stream Mach number
p_b	Model base pressure (average of 4 taps)
P_b	Base pressure coefficient = $\frac{p_b - p_\infty}{q}$
p_c	Cone surface pressure (measured 0.60 in. ahead of base)
p_∞	Free stream static pressure
q	Dynamic pressure = $\frac{1}{2}\rho V^2$
r	Nose radius of blunted cone
R	Base radius of cones
Re_L	Reynolds number based on wetted length and local conditions at outer edge of boundary layer just ahead of base of body
Re_∞	Reynolds number based on wetted length and free stream conditions
S	Model reference area = 7.069 square inches
V	Free stream air velocity
ρ	Mass density

1. INTRODUCTION

While there has been much interest in the subject of base pressure in the past several years, there has been a noticeable lack of experimental data at hypersonic velocities. Many investigators have obtained a wealth of data at velocities up to Mach 5, and there have been several semiempirical theories advanced; however, little has been done above Mach 5.

The present limited investigation was initiated in order to begin to fill the void of hypersonic base pressure data, to evaluate our ability to accurately measure low pressures, to determine the effect of Mach number, Reynolds number, and boundary layer trip devices on base pressure, and to compare our test results with other experimental data, at least at the lower Mach numbers.

The present tests were considered a success, and further tests on bodies of different shapes are being planned.

2. MODELS AND APPARATUS

2.1 Wind Tunnels

The tests were conducted in Supersonic Wind Tunnel No. 1 and Hypersonic Wind Tunnel No. 4. The supersonic tunnel is of the continuous flow, closed circuit, variable density type and has a flexible nozzle for obtaining a range of Mach numbers from 1.50 to 5.00. The test section size is 13 inches wide by 15 inches high. The hypersonic tunnel is of the continuous flow, open jet, closed circuit, variable density variety. It has interchangeable axisymmetric nozzles for Mach numbers 6.0, 7.5, and 9.2 with exit diameters of 14.6, 15.6, and 18.7 inches, respectively. A combustion and an electric heater provide stagnation temperatures up to 1960° Rankine--sufficient to prevent air liquefaction. The specific humidity was maintained at a value less than 0.0002 lb of water vapor per pound of air for all tests. Further information on the tunnels may be found in Ref. 1.

2.2 Instrumentation

The base pressures were transmitted to four 0-1 psi Statham absolute pressure transducers which were located outside the test section. The sensitivity of the transducers was increased by using a supply voltage of 6.0 volts rather than the design voltage of 3.5 volts. The transducers then had a range

of 0-0.6 psia with an accuracy of better than ±0.25 percent of their range. The cone pressure was measured on a 0-5 psi Statham absolute pressure transducer whose sensitivity had been increased to give it a 0-3 psi range. Its accuracy was also better than ±0.25 percent of its range. The transducers were zero referenced to a vacuum system which measured less than 0.025 mm Hg at all times.

The electrical signals from the transducers were converted by the automatic data readout system to proportional digital readings which were typed on data sheets and punched in code on a tape. A schlieren system with camera provided continuous visual indication, as well as photographs, of the flow conditions in the test section. Spark shadowgraph photos were also taken.

2.3 Models

The models tested were sharp and hemispherically blunted 9° half angle cones. They were tested both with and without a square trip ring of height and width 0.050 inch, which had an inside diameter of 1.25 inches. The purpose of the trip ring was to artificially induce a turbulent boundary layer on the model. The sharp nose model was 9.471 inches long and had a 3.000-inch base diameter. The blunt nosed model used the same base and was 7.160 inches long. It had a nose radius of 0.429 inch. There were four base pressure taps located on a vertical diameter at varying distances from the model axis. One cone surface pressure tap was located on the top of the model, 0.600 inch from the base. The model physical characteristics are illustrated in the drawing, Figure 1.

3. TEST PROCEDURE

With the model installed on the tunnel centerline, flow was established at the desired Mach number, but at reduced stagnation pressure and temperature. Next, pressure and temperature were increased to their proper value for the test, and schlieren and shadowgraph photographs were taken. Then, pressure data were taken at one minute intervals until there was no noticeable change in pressure with time. After that, tunnel flow conditions were changed and the process repeated. Data were taken at zero angle of attack only.

4. DATA REDUCTION

4.1 Procedure

The raw numerical data from the typed data sheets were reduced to gage pressure by using the measured transducer calibration constants. The reference pressure was then added to these values to yield absolute pressures. The four base pressure readings were averaged arithmetically to yield an average base pressure, p_b. This pressure was reduced to coefficient form by subtracting from it the test section static pressure, p_∞, and then dividing the difference by the dynamic pressure, q. The local Reynolds number, Re_L, was obtained by determining the local Mach number at the base of the model and then using Chart 25 in NACA Report 1135, using stagnation conditions in the case of the sharp cone and total conditions behind a normal shock in the case of a blunt cone.

4.2 Accuracy

The maximum deviation of any of the measured base pressures from the average values does not exceed ±0.002 psi, which is ±0.25 percent of the range of the transducers. The cone surface pressure readings were reduced in a similar manner and were also found to be consistent with transducer accuracy. The maximum error in base pressure coefficient due to transducer inaccuracy is ±.0025. The range of p_b measured was from 0.0035 to 0.165 psia.

5. PRESENTATION OF DATA

The data from the wind tunnel tests are presented in several different ways in order to better illustrate certain trends, and to compare with the theoretical and experimental work of others.

In Figs. 2-5, the base pressure coefficient, P_b, is plotted as a function of free stream Reynolds number, Re_∞, based on model wetted length. Each figure is for a different configuration, with a curve for each Mach number. In Figs. 6-12, we also plot P_b vs Re_∞; however, in these, each figure is for a different Mach number, with a curve for each configuration.

In Figure 13, P_b is plotted versus local Reynolds number, Re_L, based on conditions just outside the boundary layer at the model base and the model

wetted length. The points plotted are for cases where boundary layer transition has occurred before the model base. Each curve is for a different Mach number.

Fig. 14 shows the present data for sharp and blunt cones, without trip rings, plotted as a ratio of base pressure to cone surface pressure, P_b/P_c, vs Re_L. This is compared to data of Whitfield and Potter from Ref. 2, which is also for flow over sharp and blunt 9° cones. Fig. 15 is similar to Fig. 14, the only difference being that the present data shown are for models with the trip ring. It is again compared to Whitfield and Potter's data which are for models without boundary layer tripping devices.

Fig. 16 shows P_b plotted as a function of free stream Mach number, M_∞. The points shown are for a sharp cone with a trip ring at a free stream Reynolds number of 6×10^6. The data are compared to a compilation by Chapman, found in Ref. 3, for flow over axisymmetric models with cylindrical afterbodies and data for a 3/4 power law body from Ref. 4 by Reller and Hamaker.

In Figs. 17 and 18, drag coefficient is plotted against Mach number for the sharp and blunt cones, respectively. The contributions of base and wave drag are compared. The contribution of friction drag is small and has been neglected.

Fig. 19 shows the ratio of base pressure to free stream static pressure plotted as a function of free stream Mach number. An "approximate estimate" from Ref. 2 for a 9° blunt cone with $r/R = 0.3$ and $Re_L \geq 40 \times 10^6$ is compared to present data where the cone angle is 9°, $r/R = 0.286$ and Re_L is sufficient to insure a turbulent boundary layer on the model.

6. DISCUSSION OF RESULTS

In Figs. 2-5, we see the effect of free stream Reynolds number and Mach number on the base pressure coefficient for the different configurations tested. We can see that, with increasing Reynolds number, the base pressure coefficient decreases (becomes more negative), and the base drag increases. This is due to the fact that at the higher Reynolds number the boundary layer becomes turbulent on the body and improves the mixing in the base region.

The base pressure coefficient increases with increasing Mach number, and the base drag therefore decreases.

The difference between the sharp and blunt cones and the effect of the boundary layer trip ring can best be seen in Figs. 6-12. Here we see that transition and the values of P_b characteristic of turbulent boundary layers occur at lower values of Re_∞ for the models with the trip ring. We may also note that once turbulent flow on the model is obtained, there is very little dependence on whether transition occurred naturally or by means of the trip ring. This is more evident in the case of the sharp cone since, at some of the Mach numbers tested, it was not possible to obtain turbulent flow on the blunt cone without the trip ring.

Fig. 13, which shows P_b plotted against local Reynolds number, shows that, for the turbulent data, an empirical correlation between the sharp and blunt cones is possible. For the present tests, the equation

$$-P_b = 0.00483 \log Re_L + k$$

best describes the data, where "k" varies with Mach number as follows:

M	k
3.50	0.0643
4.00	0.0445
4.50	0.0289
5.00	0.0158
6.00	0.0033
7.50	-0.0102
9.20	-0.0157

Fig. 14 shows the ratio of base pressure to cone pressure plotted as a function of local Reynolds number for sharp and blunt cones without trip rings. In addition to the present data, those of Whitfield and Potter, found in Reference 2, are also plotted. From the discussion of Figures 2-5 and from Figure 14, it is clear that local Reynolds numbers for the present tests were not high enough to produce a turbulent boundary layer over the model in the majority of cases. In the cases where there were turbulent boundary layers in both the present tests and those of Ref. 2, agreement between the two sets

of data is fairly good. The difference is primarily that of transition Reynolds number. This can be explained by the fact that model surface roughness and tunnel turbulence level, which are undoubtedly different for the two sets of data, have a significant effect.

In Fig. 15, which is similar to Fig. 14, the present data for the models with the trip ring are compared to those of Whitfield and Potter without a tripping device. The present data seem to level off to values fairly close to the higher Reynolds number data of Whitfield and Potter. Little more can be said about this data, due to the very large scatter. This scatter is believed to be due to the inability to obtain very high Reynolds numbers. Thus, it fixes transition well forward of the base on the model.

Fig. 16 shows base pressure coefficient as a function of Mach number. Present data on the sharp cone with trip ring, at Re_L of 6×10^6, is compared to compilations by Chapman and Love, found in Refs. 3 and 5, respectively, for axisymmetric models with cylindrical afterbodies. Data from Ref. 4, by Reller and Hamaker on a model with a 3/4 power law shape, is also shown. The present data compares quite well with the Chapman and Love curve at Mach 5.0 and above. Below Mach 5.0, there is good agreement between present tests and the work of Reller and Hamaker. The difference between the present data and the Chapman and Love compilation may be explained by the fact that all of their data were for models with cylindrical afterbodies. The base pressure on a cone would naturally be lower than that on a model with a cylindrical afterbody. The close agreement between the present data and the data of Reller and Hamaker on the 3/4 power law body serves to illustrate this point.

Figs. 17 and 18 show the drag contributions for the sharp and blunt cones, respectively. Friction drag was found to be small and was considered negligible. The pressure, or "fore," drag contribution was calculated by inviscid cone theory for the sharp cone, and by modified Newtonian theory for the blunt cone. The base drag was obtained from the present data for turbulent flow, for both sharp and blunt configurations.

For the sharp cone at M = 3.5, base drag is about 57 percent of the total drag, while at M = 9.2 it is only 19 percent of the total drag. In the case

of the blunt cone, these percentages are 41 and 7 percent, respectively. Thus, we see that for the more slender, streamlined shapes, base pressure is extremely important.

Figure 19 shows the ratio of base pressure to free stream static pressure plotted versus free stream Mach number. Present data for a blunt 9° cone with $r/R = 0.286$ and Re_L, sufficiently large for a turbulent boundary layer on the model, is compared to an "approximate estimate" made by Whitfield and Potter in Reference 2 for a blunt 9° cone with $r/R = 0.3$ and $Re_L \geq 40 \times 10^6$. The estimate of Whitfield and Potter was made to Mach 20 from data which went only to Mach 5.1, and the present data are in clear disagreement with it above Mach 4.5. At this Mach number and below, there is fairly good agreement between the present data and the estimate. It is felt that the estimate given in Reference 2 may lead to erroneous conclusions if used above Mach 4.5.

Further investigations on hypersonic base pressures are planned, and it is hoped that they will reinforce the present data and conclusions.

ACKNOWLEDGMENT

The author wishes to express his thanks to Mr. Robert H. Krieger, Chief, Wind Tunnel Testing Section, Supersonic Wind Tunnels Branch, for suggesting the program and for giving his invaluable help and support.

NEIL A. ZARIN

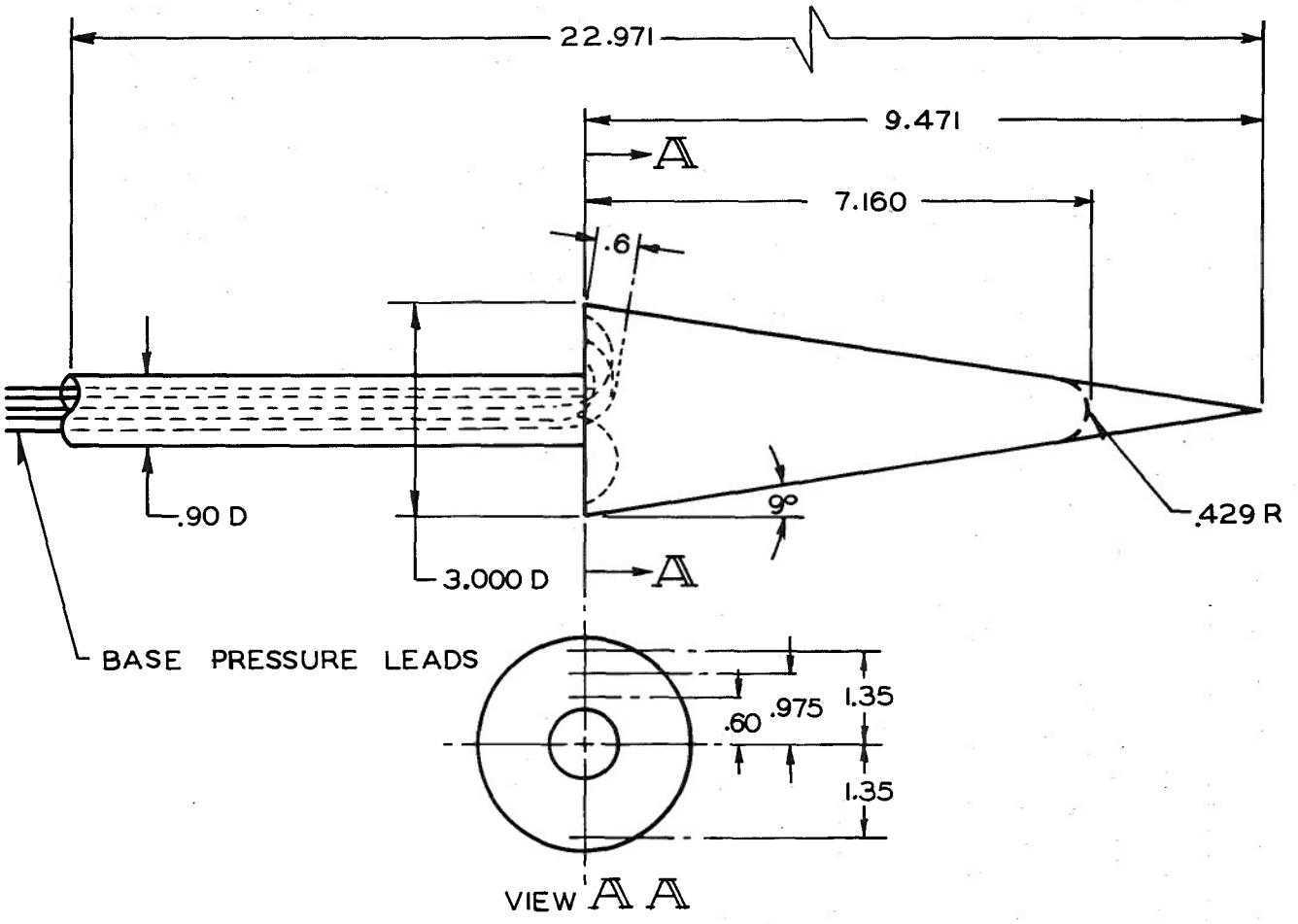

BASE PRESSURE MODELS

Fig. 1

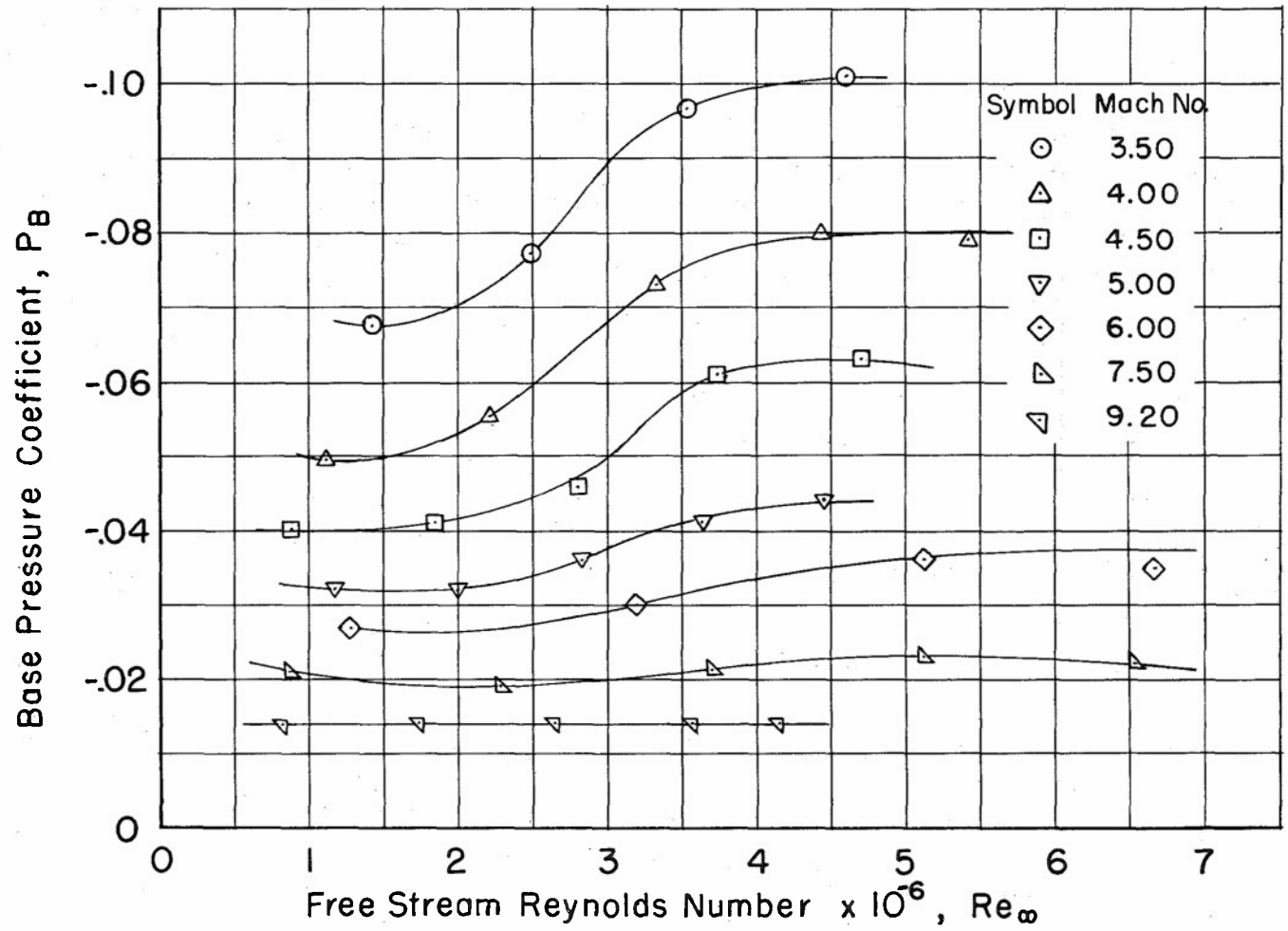

BASE PRESSURE COEFFICIENT VS. REYNOLDS NUMBER FOR A SHARP 9° CONE WITHOUT TRIP RING

Fig.2

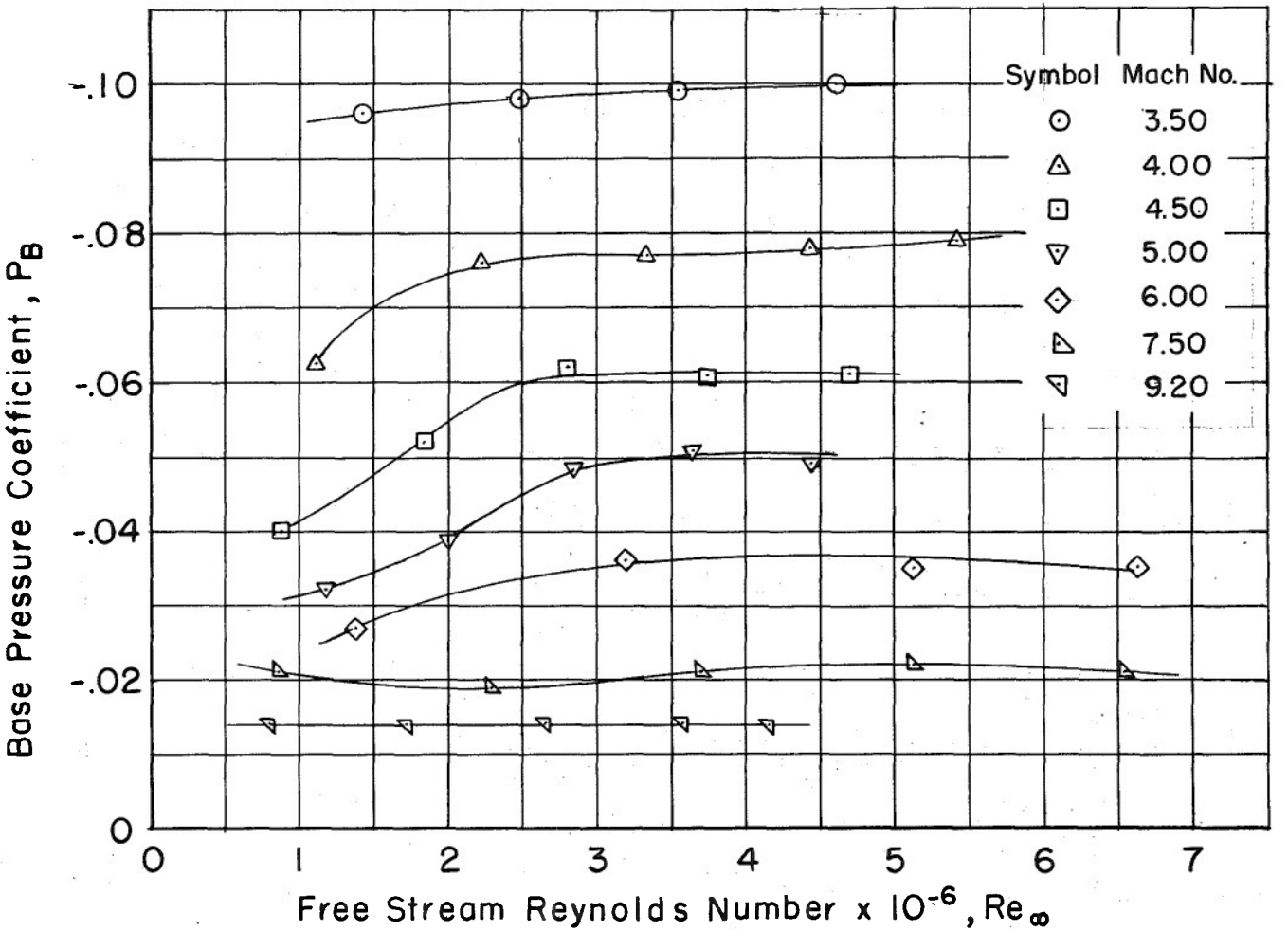

BASE PRESSURE COEFFICIENT VS REYNOLDS NUMBER FOR SHARP 9° CONE WITH BOUNDARY LAYER TRIP RING

Fig. 3

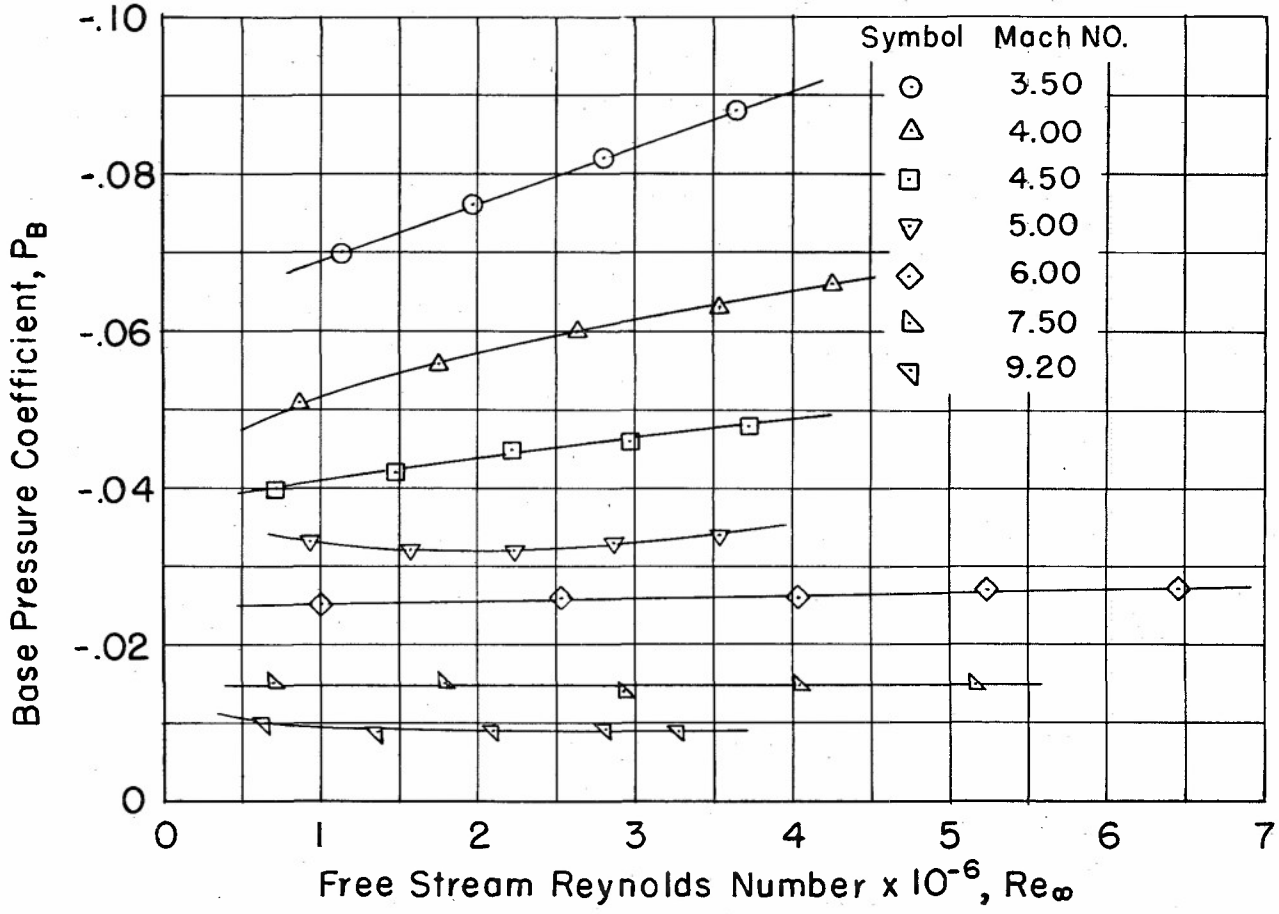

BASE PRESSURE COEFFICIENT VS FREE STREAM REYNOLDS NUMBER FOR A BLUNT 9° CONE WITHOUT TRIP RING

Fig.4

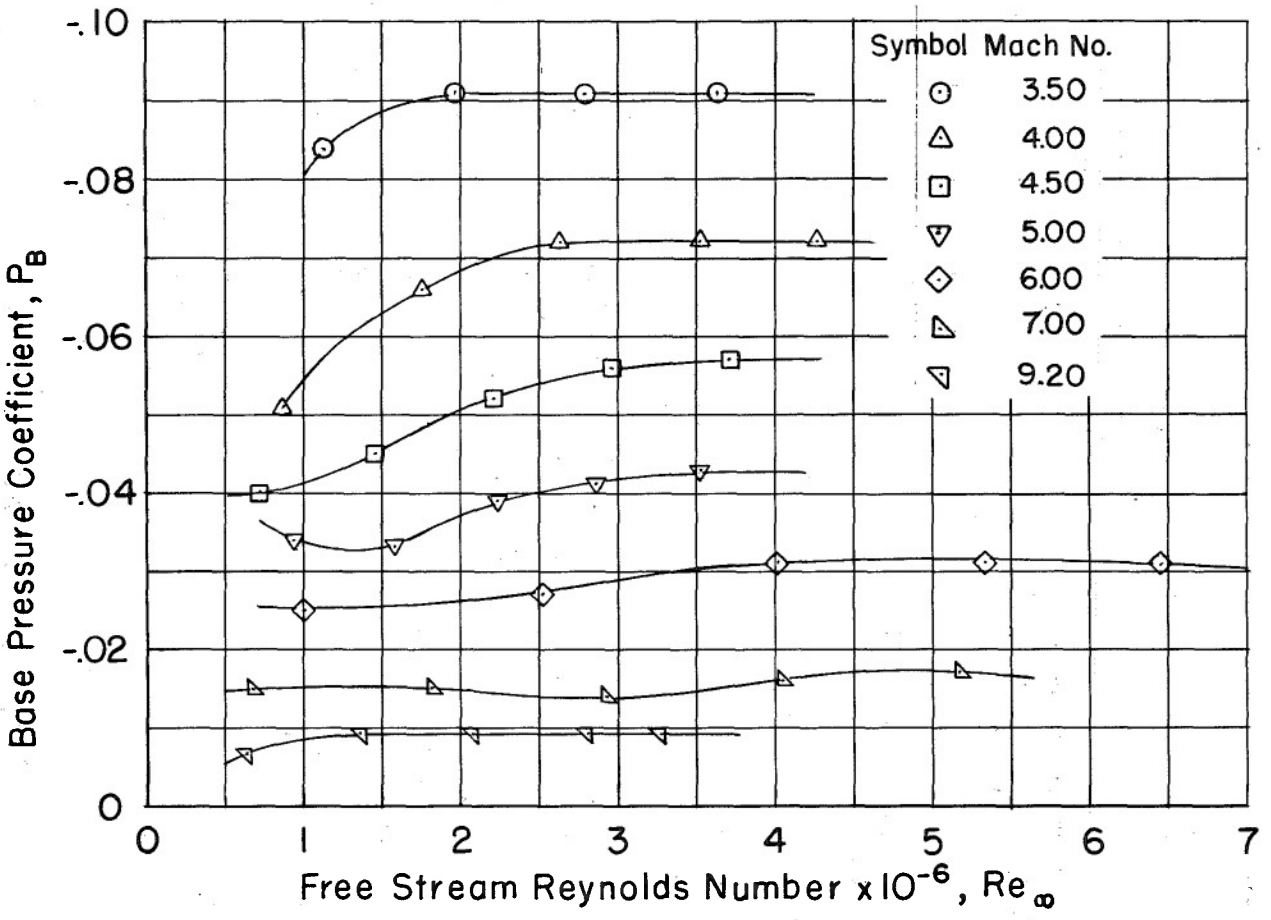

BASE PRESSURE COEFFICIENT VS REYNOLDS NUMBER FOR BLUNT 9° CONE WITH BOUNDARY LAYER TRIP RING

Fig. 5

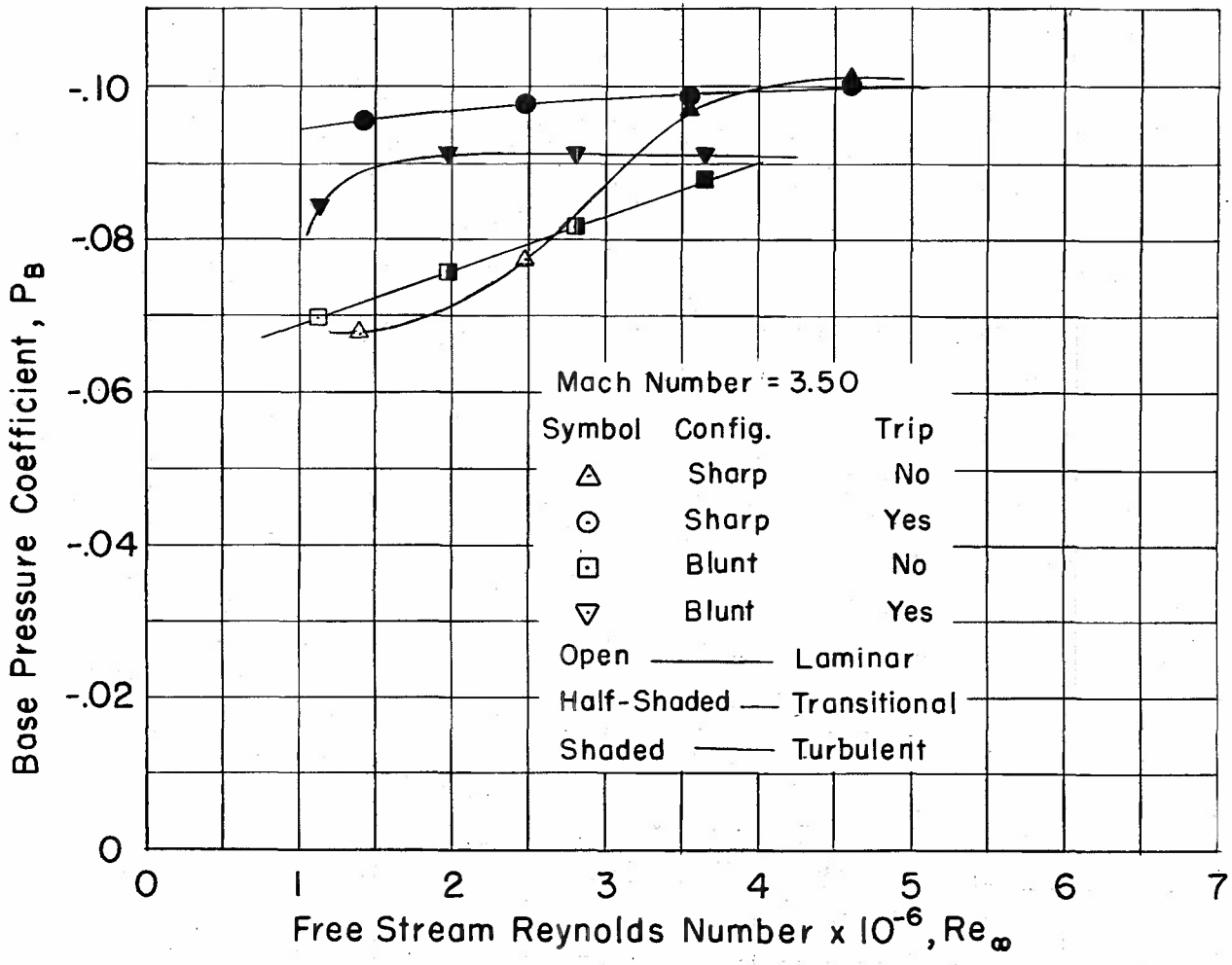

BASE PRESSURE COEFFICIENT VS REYNOLDS NUMBER

Fig. 6

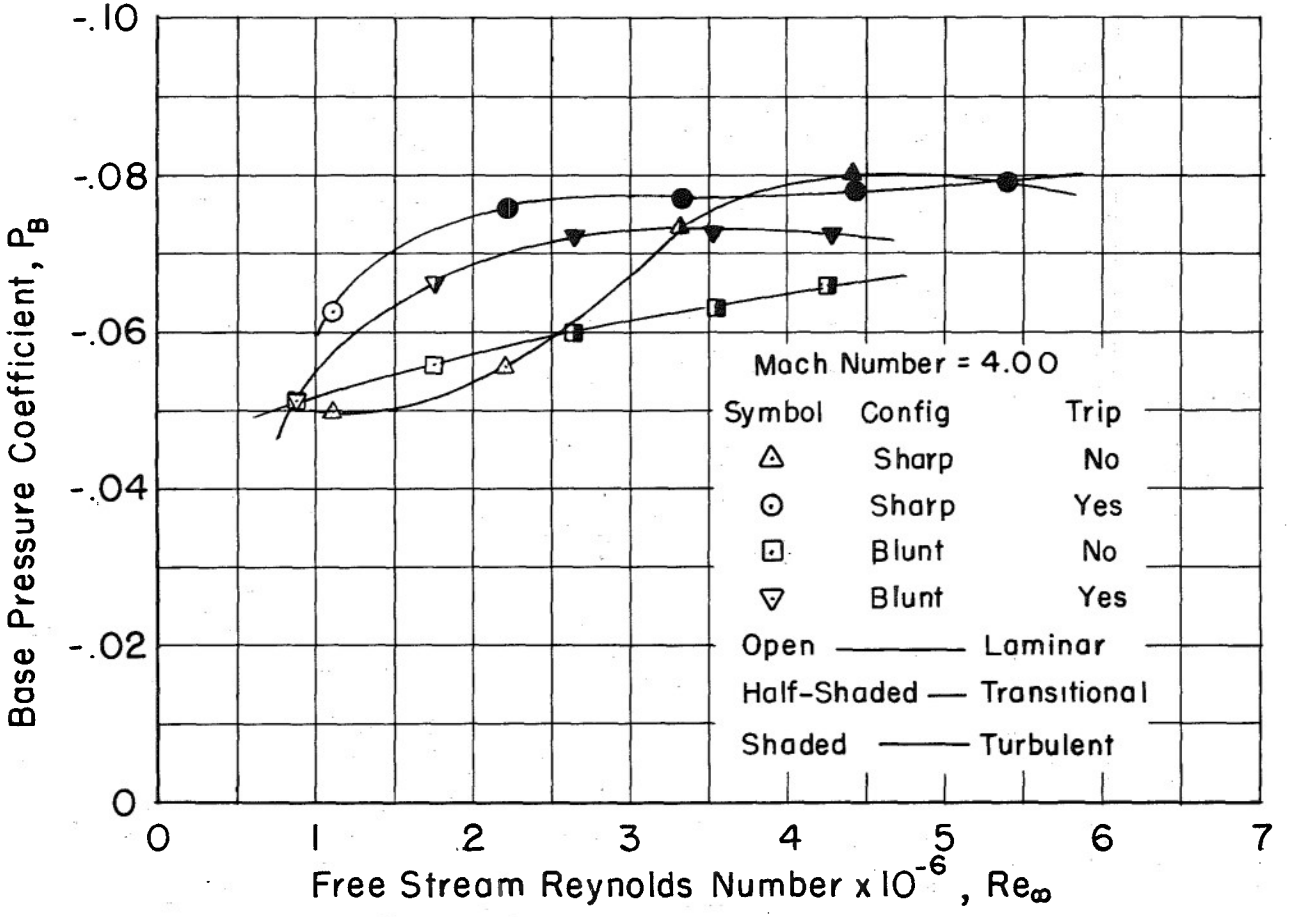

BASE PRESSURE COEFFICIENT VS REYNOLDS NUMBER

Fig. 7

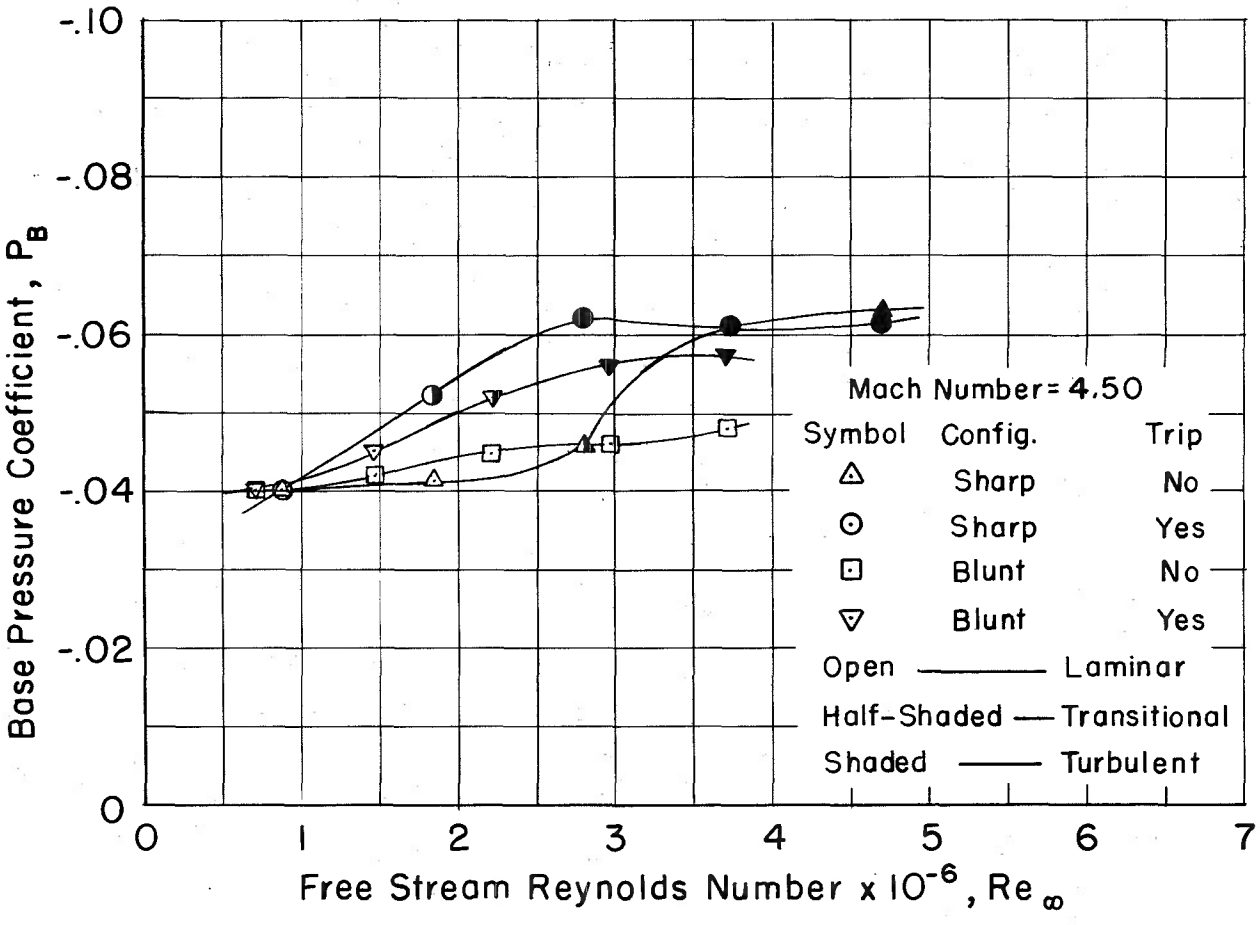

BASE PRESSURE COEFFICIENT VS REYNOLDS NUMBER

Fig. 8

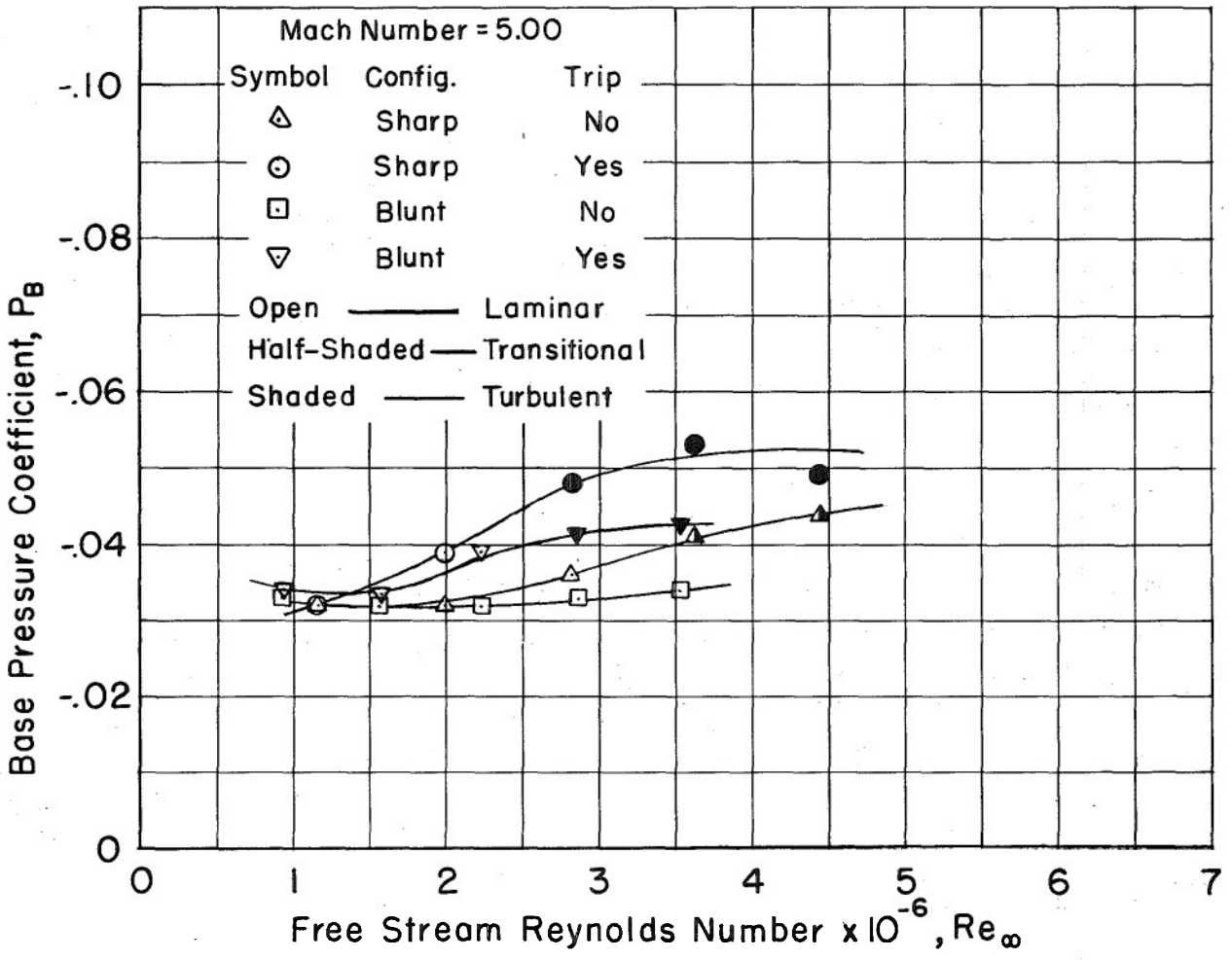

BASE PRESSURE COEFFICIENT VS REYNOLDS NUMBER

Fig. 9

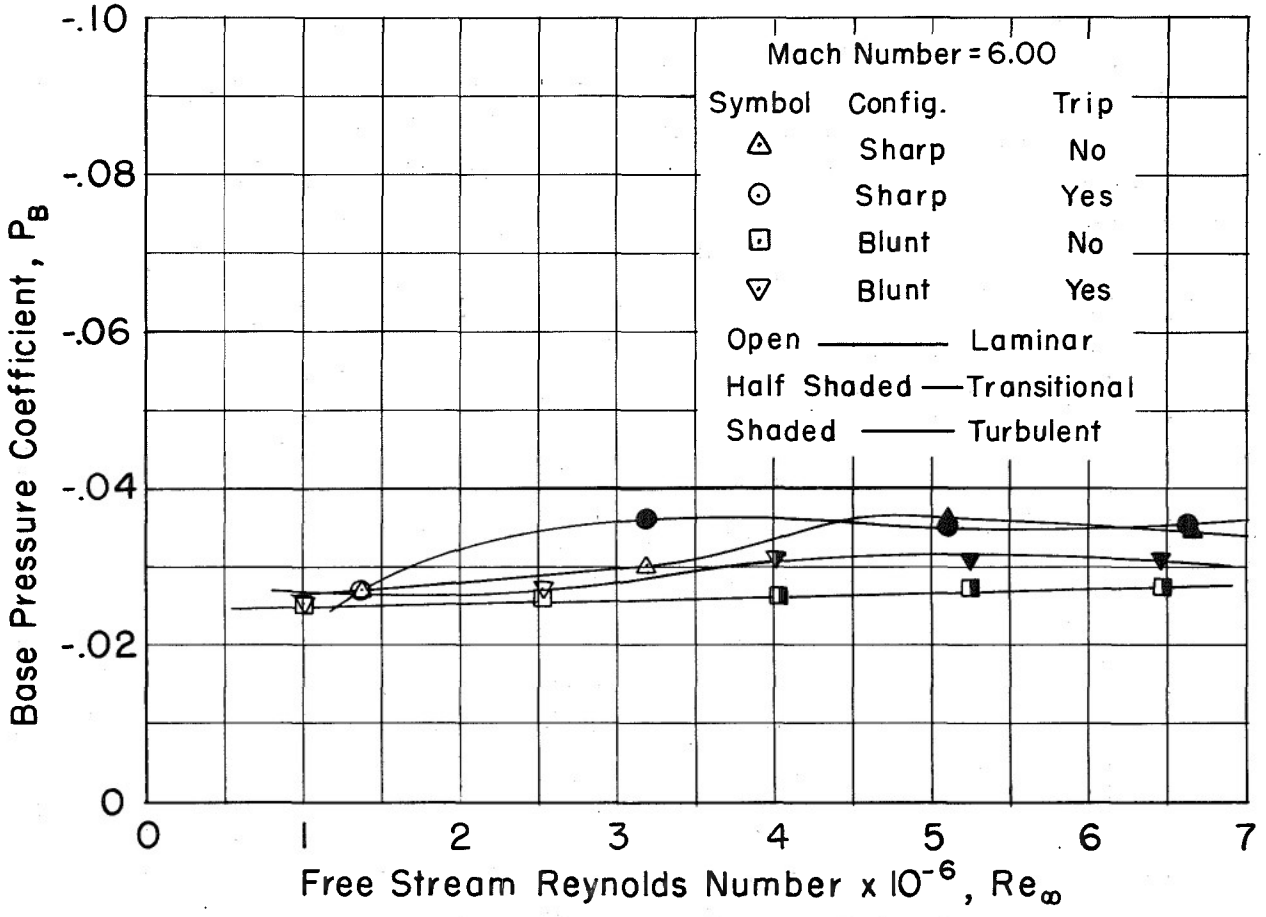

BASE PRESSURE COEFFICIENT VS REYNOLDS NUMBER

Fig.10

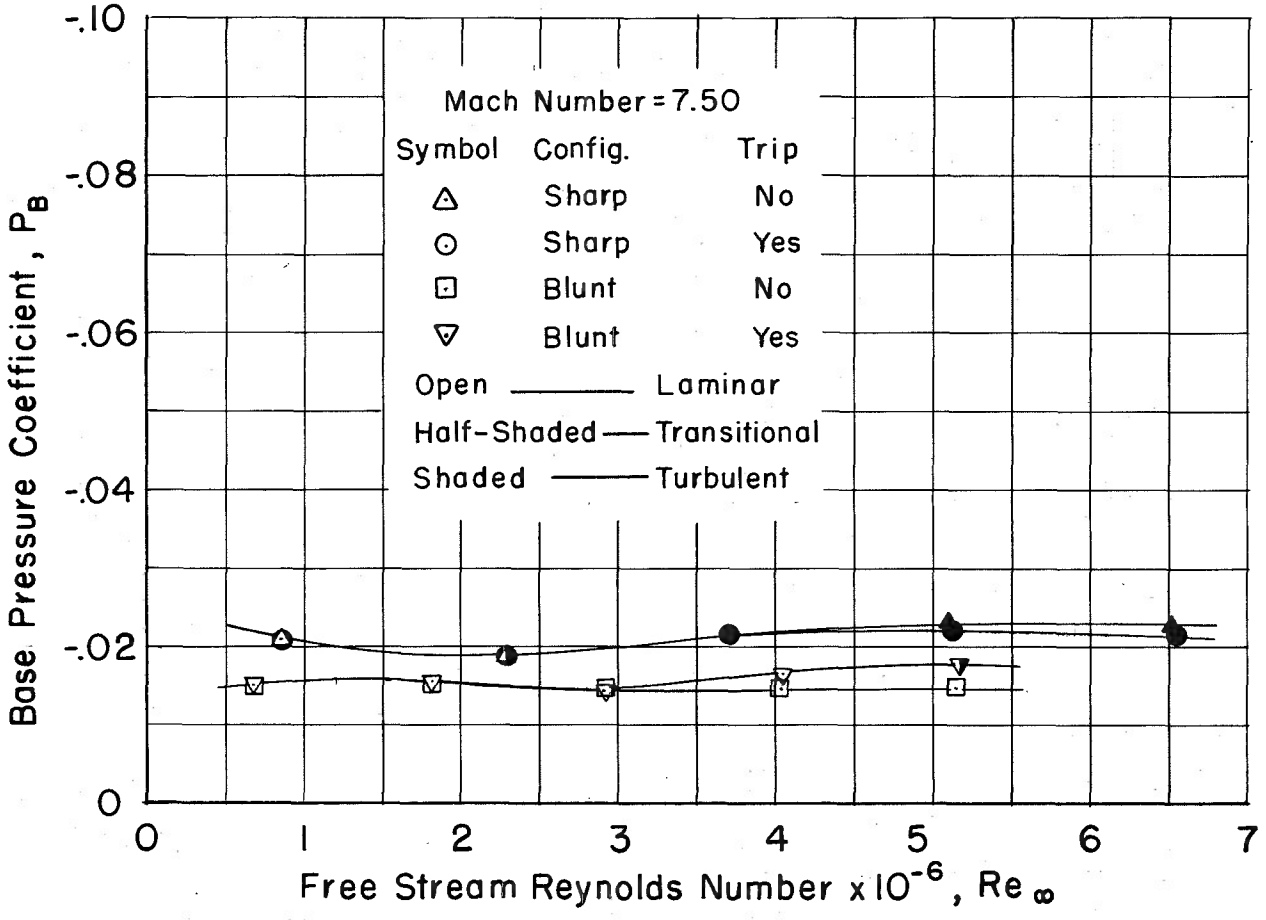

BASE PRESSURE COEFFICIENT VS REYNOLDS NUMBER

Fig. 11

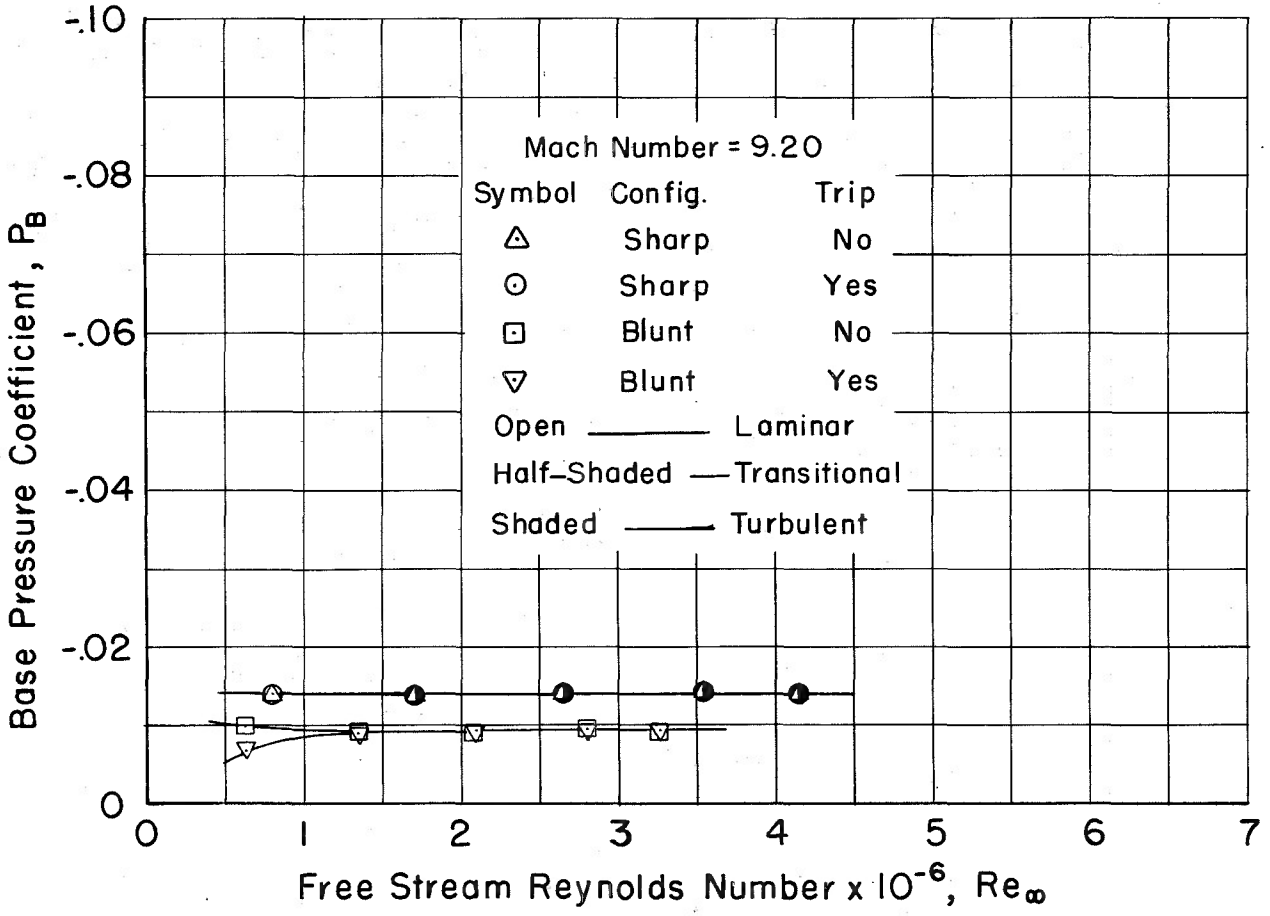

BASE PRESSURE COEFFICIENT VS REYNOLDS NUMBER

Fig.12

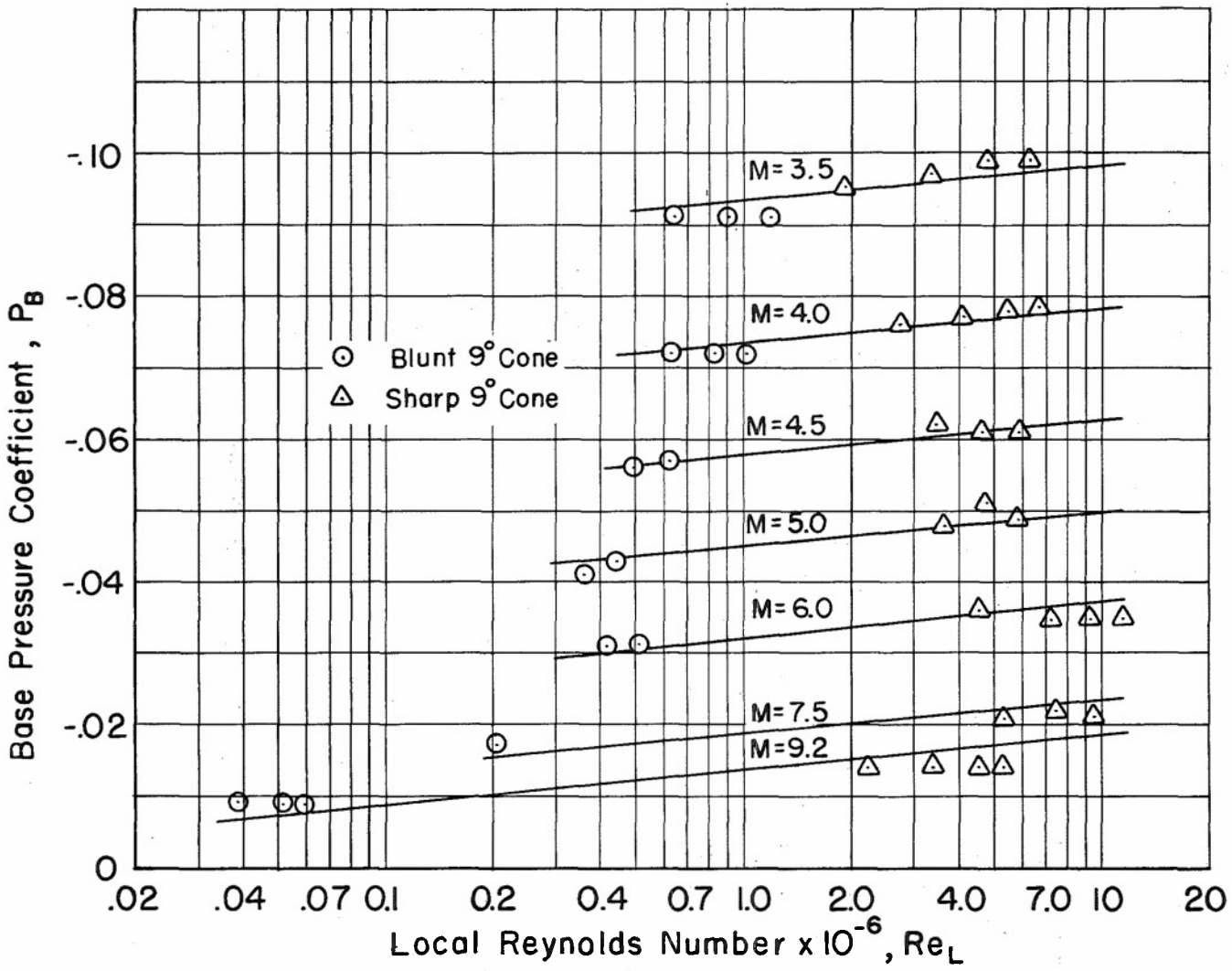

VARIATION OF BASE PRESSURE COEFFICIENT WITH LOCAL REYNOLDS NUMBER FOR RUNS WITH TURBULENT BOUNDARY LAYER ON MODEL

Fig.13

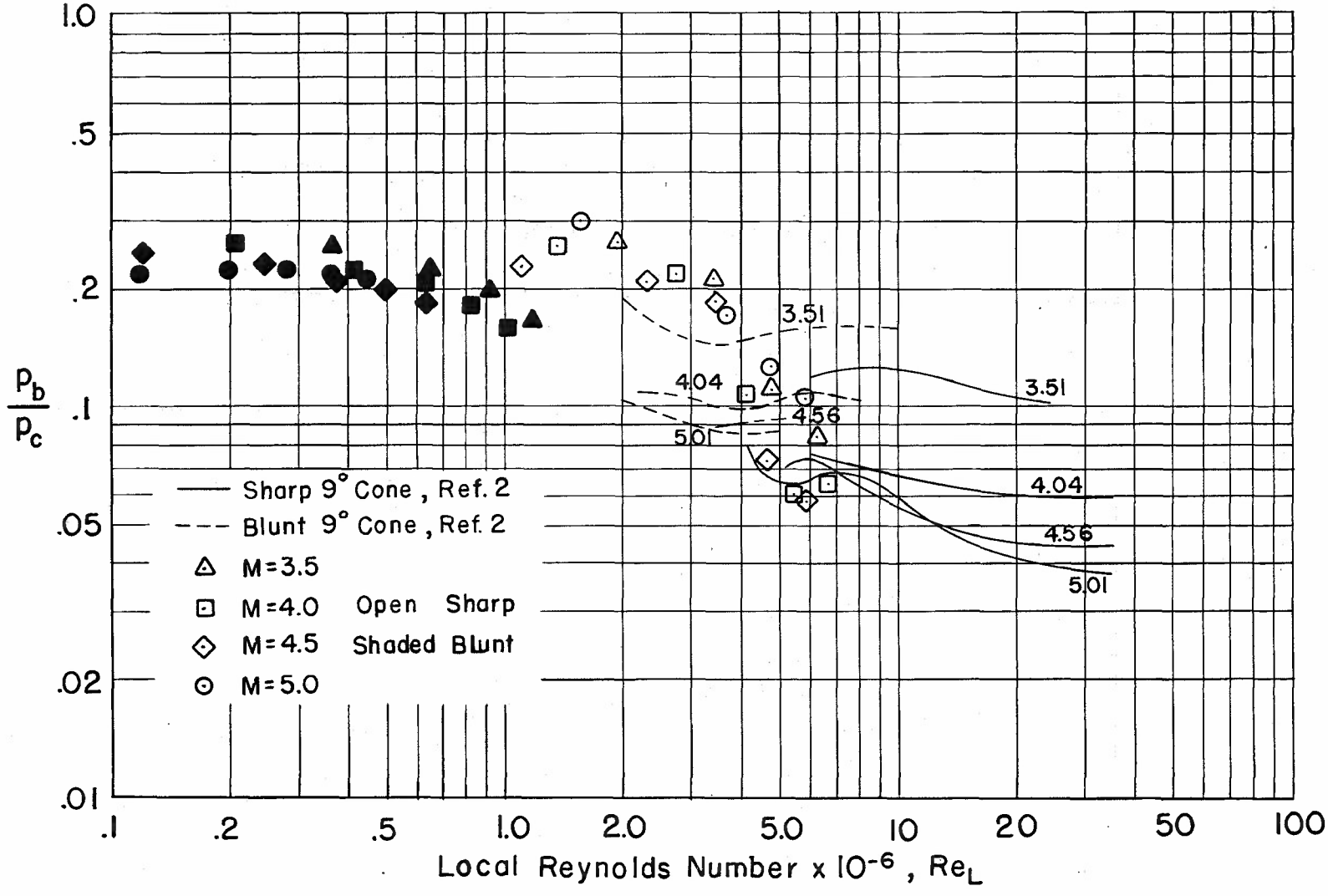

RATIO OF BASE PRESSURE TO CONE PRESSURE VS LOCAL REYNOLDS NUMBER FOR SHARP AND BLUNT 9° CONES WITHOUT TRIP RING

Fig.14

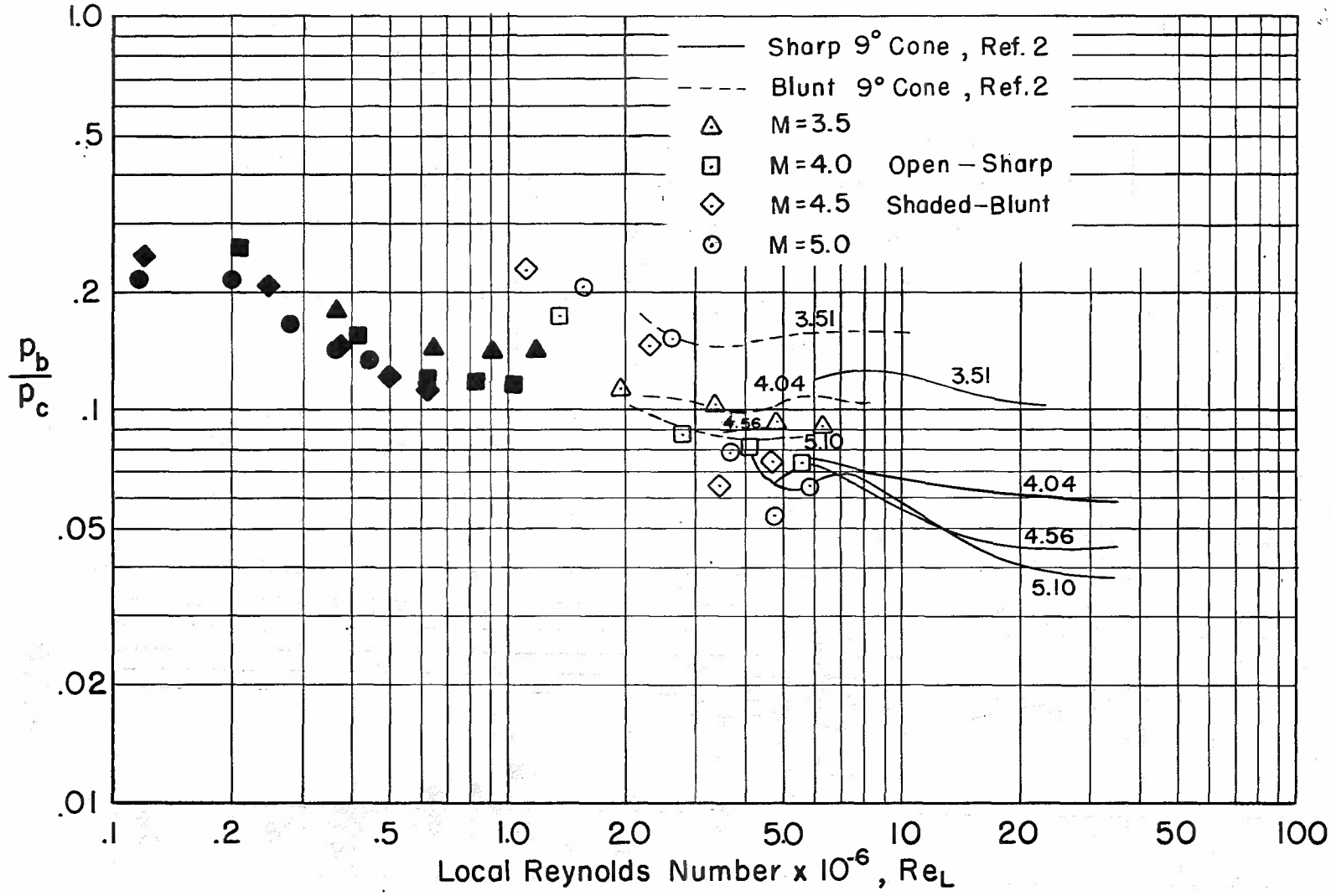

RATIO OF BASE PRESSURE TO CONE PRESSURE VS LOCAL REYNOLDS NUMBER FOR SHARP AND BLUNT 9° CONES WITH TRIP RING

Fig.15

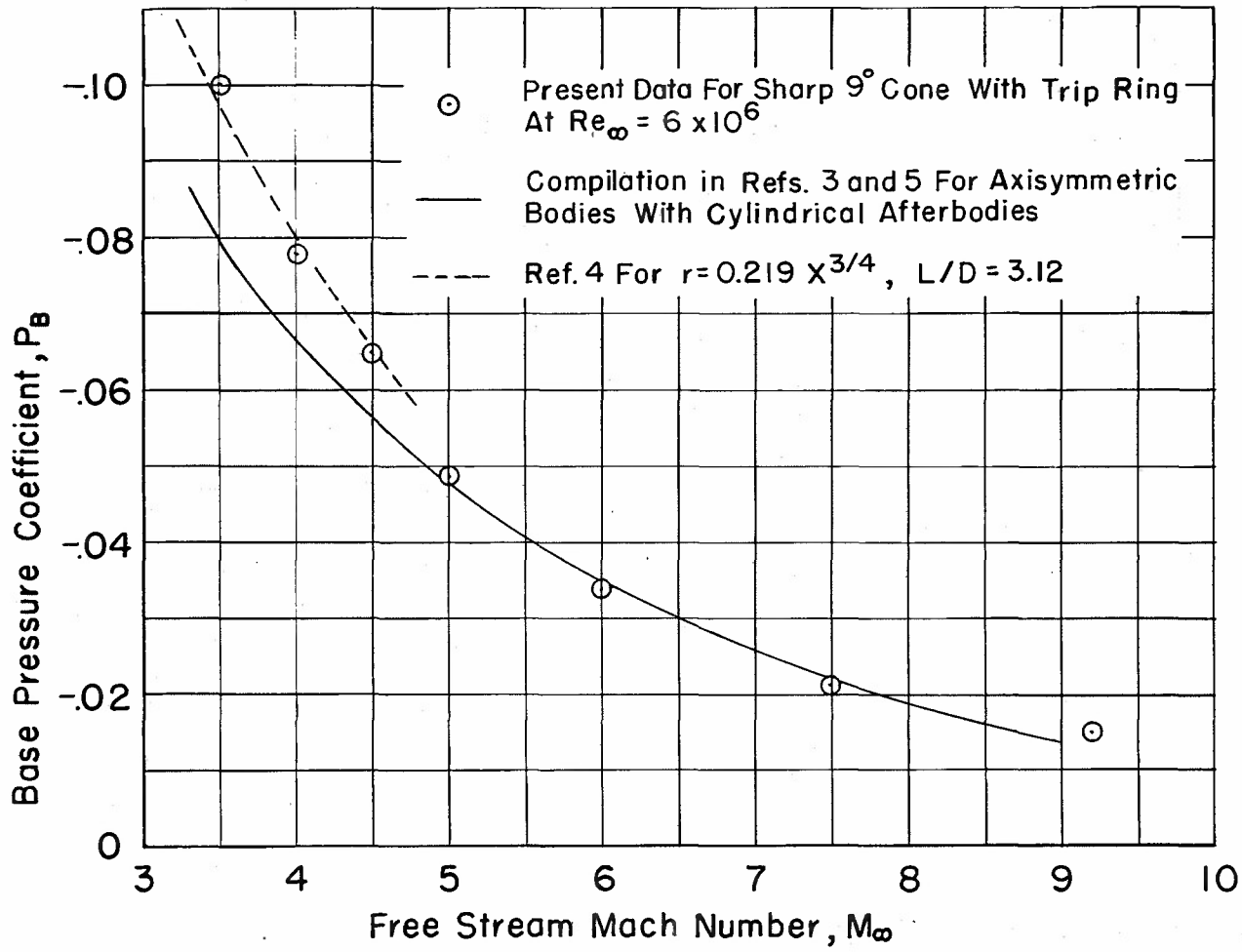

VARIATION OF BASE PRESSURE COEFFICIENT WITH FREE STREAM MACH NUMBER FOR SEVERAL NOSE SHAPES

Fig. 16

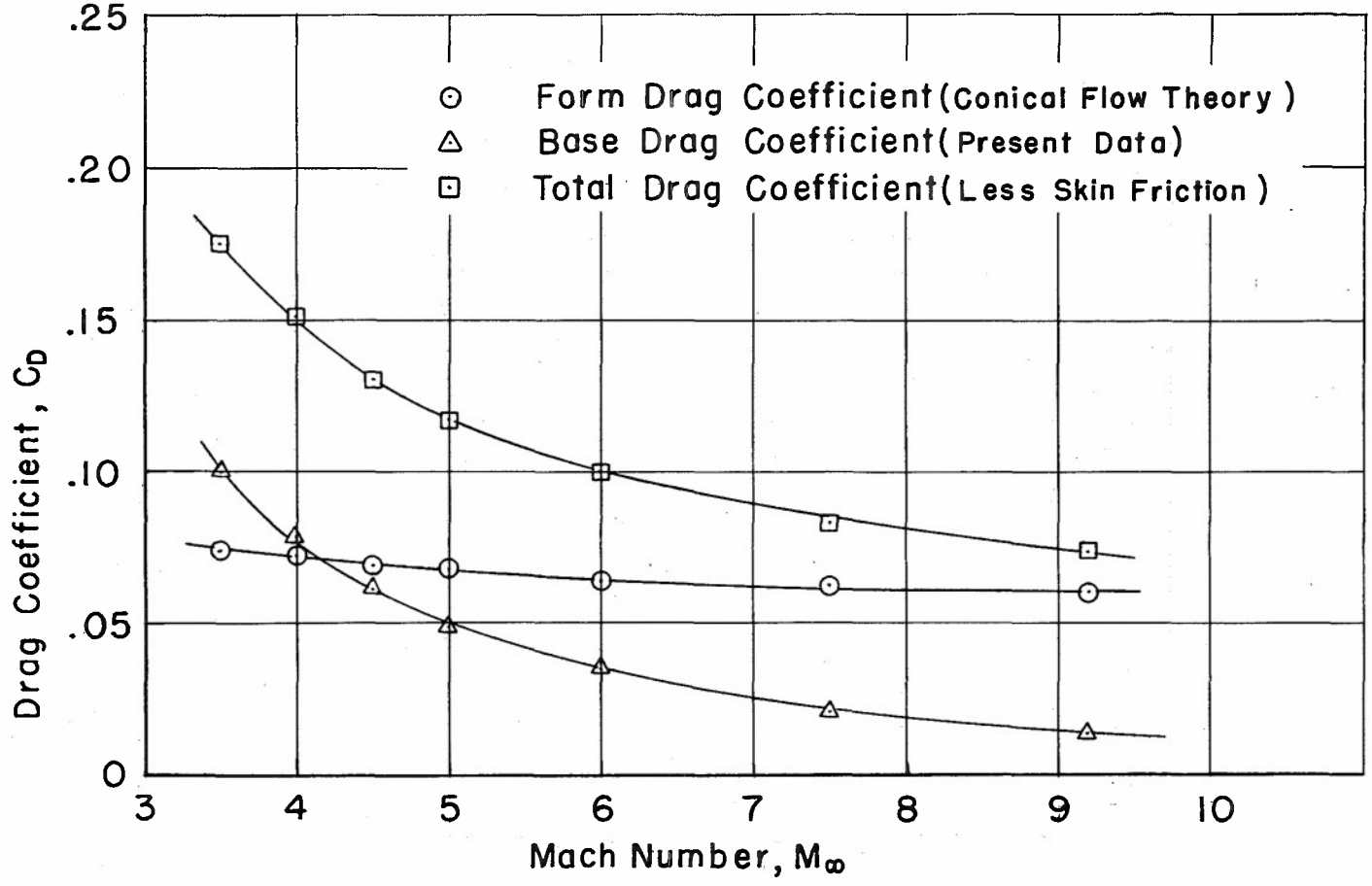

VARIATION OF DRAG COEFFICIENT WITH MACH NUMBER
FOR SHARP 9° CONE

Fig.17

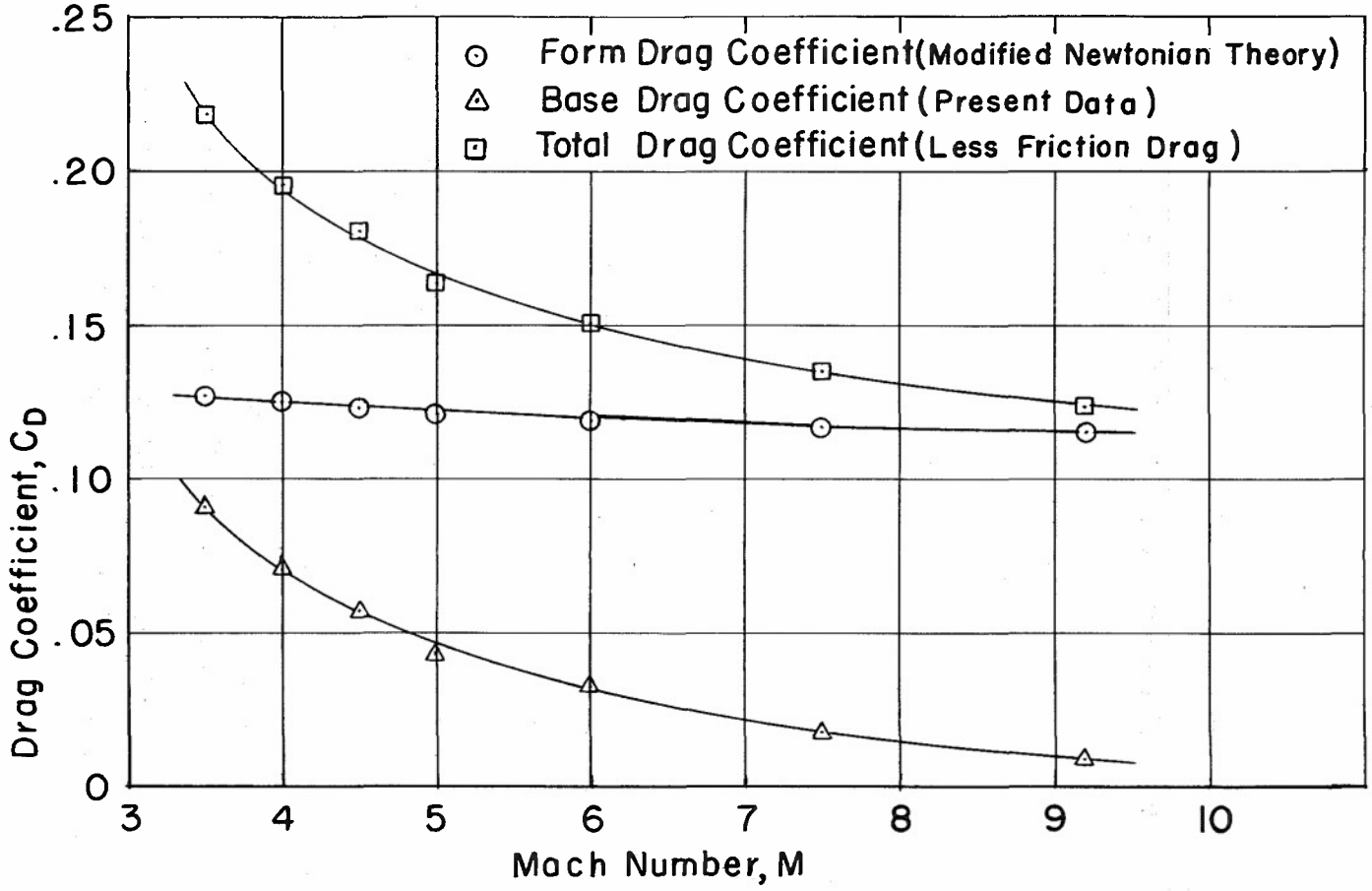

VARIATION OF DRAG COEFFICIENT WITH MACH NUMBER FOR BLUNT 9° CONE

Fig. 18

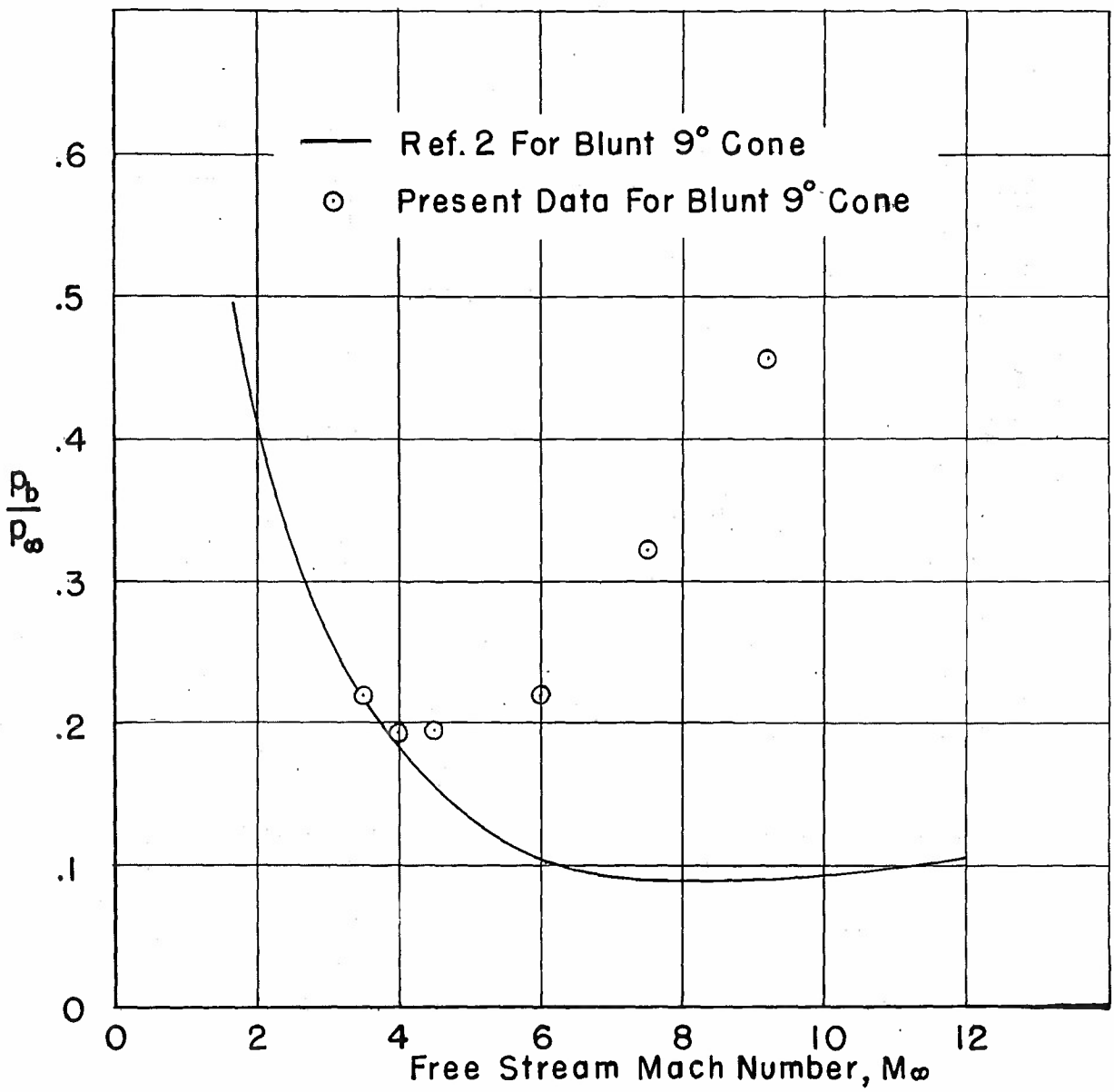

RATIO OF BASE PRESSURE TO FREE STREAM STATIC PRESSURE VS. FREE STREAM MACH NUMBER

Fig. 19

REFERENCES

1. McMullen, J. C. Wind Tunnel Testing Facilities at the Ballistic Research Laboratories. Aberdeen Proving Ground: BRL M-1292, 1960.

2. Whitfield, Jack D., and Potter, J. Leith. On Base Pressures at High Reynolds Numbers and Hypersonic Mach Numbers. AEDC TN-60-61, 1960.

3. Chapman, Dean R. An Analysis of Base Pressures at Supersonic Velocities and Comparison With Experiment. NACA Rep. 1051, 1951. (Supersedes NACA TN-2137.)

4. Reller, John O., Jr., and Hamaker, Frank M. An Experimental Investigation of the Base Pressure Characteristics of Nonlifting Bodies of Revolution at Mach Numbers from 2.73 to 4.98. NACA TN-3393, 1955.

5. Love, Eugene S. Base Pressure at Supersonic Speeds on Two-dimensional Airfoils and on Bodies of Revolution, With and Without Fins, Having Turbulent Boundary Layers. NACA TN-3819, 1957.

DISTRIBUTION LIST

No. of Copies	Organization
20	Commander Defense Documentation Center ATTN: TIPCR Cameron Station Alexandria, Virginia 22314
1	Director of Research and Laboratories HQ, U.S. Army Materiel Command Washington, D.C. 20315
1	Commanding General U.S. Army Materiel Command ATTN: AMCRD-RP-B Washington, D.C. 20315
5	Commanding General U.S. Army Missile Command ATTN: Mr. R. E. Becht AMSMI-RFSK (4 cys) Mr. R. Deep Redstone Arsenal, Alabama 35809
2	Director Redstone Scientific Information Center ATTN: Ch, Docu Sec U.S. Army Missile Command Redstone Arsenal, Alabama 35809
1	Commanding Officer U.S. Army Engineer Research & Development Laboratories ATTN: STINFO Div Fort Belvoir, Virginia 22060
1	Commanding General U.S. Army Munitions Command Dover, New Jersey 07801
2	Commanding Officer U.S. Army Frankford Arsenal ATTN: Lib Br, 0270, Bldg 40 Philadelphia, Pennsylvania 19137
3	Commanding Officer U.S. Army Picatinny Arsenal ATTN: Feltman Research Labs Mr. A. Loeb Mr. S. Wasserman Dover, New Jersey 07801
1	Commanding Officer U.S. Army Combat Developments Command Air Defense Agency Fort Bliss, Texas 79916
1	Commanding Officer U.S. Army Research Office (Durham) Box CM, Duke Station Durham, North Carolina 27706
3	Chief, Bureau of Naval Weapons ATTN: DLI-3 Washington, D.C. 20360
1	Commander U.S. Naval Ordnance Laboratory ATTN: Dr. K. Lobb White Oak Silver Spring, Maryland 20910
2	Commander U.S. Naval Ordnance Test Station ATTN: Tech Lib China Lake, California 93557
1	Commander U.S. Naval Weapons Laboratory Dahlgren, Virginia 22448

DISTRIBUTION LIST

No. of Copies	Organization
1	Superintendent U.S. Naval Postgraduate School ATTN: Tech Rept Sec Monterey, California 93940
2	Director U.S. Naval Research Laboratory ATTN: Tech Info Div Mr. Walter Atkins Washington, D.C. 20390
1	AEDC (AER) Arnold AFS Tennessee 37389
1	APGC (PGBPS-12) Elgin AFB Florida 32542
1	SEG (SERDA) Wright-Patterson AFB Ohio 45433
1	AFFDL Wright-Patterson AFB Ohio 45433
1	Director U.S. National Bureau of Standards ATTN: G. B. Schubauer Connecticut Ave. & Van Ness St., N.W. Washington, D.C. 20235
1	Applied Physics Laboratory The Johns Hopkins University 8621 Georgia Avenue Silver Spring, Maryland 20910
1	Director Scientific and Technical Information Facility ATTN: NASA Rep (ATS) P.O. Box 5700 Bethesda, Maryland 20014
2	Director National Aeronautics and Space Administration Ames Research Center ATTN: H. J. Allen Tech Lib Moffett Field, California 94035
1	Director Jet Propulsion Laboratory ATTN: W. Howard 4800 Oak Grove Drive Pasadena, California 91103
2	Director National Aeronautics and Space Administration Langley Research Center ATTN: Mr. C. E. Brown Tech Lib Langley Station Hampton, Virginia 23365
2	Director National Aeronautics and Space Administration Lewis Research Center ATTN: Tech Lib 21000 Brookpark Road Cleveland, Ohio 44135
6	Director National Aeronautics and Space Administration George C. Marshall Space Flight Center ATTN: Mr. E. B. May Mr. C. D. Andrews R-AERO-ADE Tech Lib, MS-IPL Huntsville, Alabama 35812
1	Gas Dynamics Facility ARO, Inc. ATTN: Mr. J. Lukasiewicz Tullahoma, Tennessee 37388

DISTRIBUTION LIST

No. of Copies	Organization
1	The Martin Company ATTN: Dr. M. Morkovin Baltimore, Maryland 21203
1	Case Institute of Technology ATTN: Mr. R. Bolz 10900 Euclid Avenue Cleveland, Ohio 44106
1	Massachusetts Institute of Technology Naval Supersonic Laboratory ATTN: Mr. Frank R. Durgin 560 Memorial Drive Cambridge, Massachusetts 02139
1	Southwest Research Institute Department of Applied Mechanics ATTN: Mr. W. Squire 8500 Culebra Road San Antonia, Texas 78228
1	Stanford University Aerodynamics Department ATTN: W. G. Vincenti Stanford, California 94305
1	University of Texas Defense Research Laboratory ATTN: Mr. J. B. Oliphint 500 E. 24th St. Austin, Texas 78712
1	Professor S. Bogdonoff Forrestal Research Center Princeton University Princeton, New Jersey 08540
1	Professor G. F. Carrier Harvard University Cambridge, Massachusetts 01938
1	Professor F. H. Clauser, Jr. Department of Aeronautics The Johns Hopkins University Baltimore, Maryland 21218
1	Professor Harold de Groff School of Aeronautical Engineering Purdue University Lafayette, Indiana 47907
2	Professor L. Lees Guggenheim Aeronautical Laboratory California Institute of Technology Pasadena, California 91004
1	Professor M. Lesson Department of Aeronautical Engineering Pennsylvania State University State College, Pennsylvania 16801
1	Professor H. W. Liepmann Aeronautics Department California Institute of Technology Pasadena, California 91102
1	Professor H. S. Stillwell Department of Aeronautical Engineering University of Illinois Urbana, Illinois 61803
1	Professor R. E. Street Department of Aeronautical Engineering University of Washington Seattle, Washington 98105

DISTRIBUTION LIST

No. of Copies	Organization
1	Professor G. L. von Eschen Aeronautical Engineering Department Ohio State University Columbus, Ohio 43210
1	Dr. S. Corrsin Department of Mechanics The Johns Hopkins University Baltimore, Maryland 21218
1	Dr. E. R. G. Eckert Department of Mechanical Engineering University of Minnesota Minneapolis, Minnesota 55414
1	Dr. Antonio Ferri Director, Aerospace Laboratory New York University 181 St. & University Ave. New York, New York 10053
1	Dr. J. V. Foa Aerodynamics Department Rensselaer Polytechnic Institute Troy, New York 12181
1	Dr. Arnold Kuethe Department of Aeronautical Engineering University of Michigan East Engineering Building Ann Arbor, Michigan 48104
1	Dr. A. E. Puckett Systems Development Laboratory Hughes Aircraft Company Culver City, California 90230
1	Dr. W. R. Sears Graduate School of Aeronautical Engineering Cornell University Ithaca, New York 14850
Aberdeen Proving Ground	
	Ch, Tech Lib
	Air Force Ln Ofc Marine Corps Ln Ofc Navy Ln Ofc CDC Ln Ofc

Unclassified
Security Classification

DOCUMENT CONTROL DATA - R&D

(Security classification of title, body of abstract and indexing annotation must be entered when the overall report is classified)

1. ORIGINATING ACTIVITY *(Corporate author)*
U.S. Army Ballistic Research Laboratories
Aberdeen Proving Ground, Maryland

2a. REPORT SECURITY CLASSIFICATION
Unclassified

2b. GROUP

3. REPORT TITLE

BASE PRESSURE MEASUREMENTS ON SHARP AND BLUNT 9° CONES AT MACH NUMBERS FROM 3.50 TO 9.20

4. DESCRIPTIVE NOTES *(Type of report and inclusive dates)*

5. AUTHOR(S) *(Last name, first name, initial)*

Zarin, Neil A.

6. REPORT DATE	7a. TOTAL NO. OF PAGES	7b. NO. OF REFS
November 1965	40	5

8e. CONTRACT OR GRANT NO.	9a. ORIGINATOR'S REPORT NUMBER(S)
b. PROJECT NO. RDT&E 1A222901A201	Memorandum Report No. 1709
c.	9b. OTHER REPORT NO(S) *(Any other numbers that may be assigned this report)*
d.	

10. AVAILABILITY/LIMITATION NOTICES

Distribution of this document is unlimited.

11. SUPPLEMENTARY NOTES	12. SPONSORING MILITARY ACTIVITY
	U.S. Army Materiel Command Washington, D.C.

13. ABSTRACT

Base pressure measurements were made on sharp and hemispherically blunted 9° cones at Mach numbers from 3.50 to 9.20. The tests were carried out in the Ballistic Research Laboratories' Supersonic and Hypersonic Wind Tunnels at Aberdeen Proving Ground, Maryland. The data obtained are compared to experimental data and to data from semiempirical analyses from other sources. An empirical correlation for the base pressure data is presented. The relative contributions of base and form drag to total drag are compared.

DD FORM 1 JAN 64 1473

Unclassified
Security Classification

14. KEY WORDS	LINK A		LINK B		LINK C	
	ROLE	WT	ROLE	WT	ROLE	WT
Base Pressure						
Supersonic						
Hypersonic						
Base Drag						
Form Drag						
Base Pressure Coefficient						
Drag Coefficient						
Cone Surface Pressure						
Reynolds Number						
Mach Number						

INSTRUCTIONS

1. ORIGINATING ACTIVITY: Enter the name and address of the contractor, subcontractor, grantee, Department of Defense activity or other organization *(corporate author)* issuing the report.

2*a*. REPORT SECURITY CLASSIFICATION: Enter the overall security classification of the report. Indicate whether "Restricted Data" is included. Marking is to be in accordance with appropriate security regulations.

2*b*. GROUP: Automatic downgrading is specified in DoD Directive 5200.10 and Armed Forces Industrial Manual. Enter the group number. Also, when applicable, show that optional markings have been used for Group 3 and Group 4 as authorized.

3. REPORT TITLE: Enter the complete report title in all capital letters. Titles in all cases should be unclassified. If a meaningful title cannot be selected without classification, show title classification in all capitals in parenthesis immediately following the title.

4. DESCRIPTIVE NOTES: If appropriate, enter the type of report, e.g., interim, progress, summary, annual, or final. Give the inclusive dates when a specific reporting period is covered.

5. AUTHOR(S): Enter the name(s) of author(s) as shown on or in the report. Enter last name, first name, middle initial. If military, show rank and branch of service. The name of the principal author is an absolute minimum requirement.

6. REPORT DATE: Enter the date of the report as day, month, year; or month, year. If more than one date appears on the report, use date of publication.

7*a*. TOTAL NUMBER OF PAGES: The total page count should follow normal pagination procedures, i.e., enter the number of pages containing information.

7*b*. NUMBER OF REFERENCES: Enter the total number of references cited in the report.

8*a*. CONTRACT OR GRANT NUMBER: If appropriate, enter the applicable number of the contract or grant under which the report was written.

8*b*, 8*c*, & 8*d*. PROJECT NUMBER: Enter the appropriate military department identification, such as project number, subproject number, system numbers, task number, etc.

9*a*. ORIGINATOR'S REPORT NUMBER(S): Enter the official report number by which the document will be identified and controlled by the originating activity. This number must be unique to this report.

9*b*. OTHER REPORT NUMBER(S): If the report has been assigned any other report numbers *(either by the originator or by the sponsor)*, also enter this number(s).

10. AVAILABILITY/LIMITATION NOTICES: Enter any limitations on further dissemination of the report, other than those imposed by security classification, using standard statements such as:

(1) "Qualified requesters may obtain copies of this report from DDC."

(2) "Foreign announcement and dissemination of this report by DDC is not authorized."

(3) "U. S. Government agencies may obtain copies of this report directly from DDC. Other qualified DDC users shall request through _____."

(4) "U. S. military agencies may obtain copies of this report directly from DDC. Other qualified users shall request through _____."

(5) "All distribution of this report is controlled. Qualified DDC users shall request through _____."

If the report has been furnished to the Office of Technical Services, Department of Commerce, for sale to the public, indicate this fact and enter the price, if known.

11. SUPPLEMENTARY NOTES: Use for additional explanatory notes.

12. SPONSORING MILITARY ACTIVITY: Enter the name of the departmental project office or laboratory sponsoring *(paying for)* the research and development. Include address.

13. ABSTRACT: Enter an abstract giving a brief and factual summary of the document indicative of the report, even though it may also appear elsewhere in the body of the technical report. If additional space is required, a continuation sheet shall be attached.

It is highly desirable that the abstract of classified reports be unclassified. Each paragraph of the abstract shall end with an indication of the military security classification of the information in the paragraph, represented as *(TS)*, *(S)*, *(C)*, or *(U)*.

There is no limitation on the length of the abstract. However, the suggested length is from 150 to 225 words.

14. KEY WORDS: Key words are technically meaningful terms or short phrases that characterize a report and may be used as index entries for cataloging the report. Key words must be selected so that no security classification is required. Idenfiers, such as equipment model designation, trade name, military project code name, geographic location, may be used as key words but will be followed by an indication of technical context. The assignment of links, rules, and weights is optional.